Electronic Supplementary Information (ESI)

Introducing an insulating alumina layer into a molecular photocathode to improve CO_2 reduction activity

Yu Takagi,[a] Masaya Yara,[b] Toshiya Tanaka,[a] Jo Onodera,[a] Minato Tanaka,[a] Megumi Okazaki,[a] Kiyoshi Miyata,[b] Ken Onda,[b] Osamu Ishitani,*[c] and Kazuhiko Maeda*[a,d]*

[a] Department of Chemistry, School of Science, Institute of Science Tokyo, 2-12-1-NE-2 Ookayama, Meguro-ku, Tokyo 152-8550, Japan.

[b] Department of Chemistry, Faculty of Science, Kyushu University, 744 Motooka, Nishi-ku, Fukuoka 819-0395, Japan.

[c] Department of Chemistry, Graduate School of Advanced Science and Engineering, Hiroshima University, 1-3-1 Kagamiyama, Higashi-Hiroshima, Hiroshima 739-8526, Japan.

[d] Research Center for Autonomous Systems Materialogy (ASMat), Institute of Science Tokyo, 4259 Nagatsuta-cho, Midori-ku, Yokohama, Kanagawa 226-8501, Japan.

*To whom corresponding authors should be addressed.

K.O.: konda@chem.kyushu-univ.jp

O.I.: iosamu@hiroshima-u.ac.jp

K.M.: maeda@chem.sci.isct.ac.jp

Experimental section

Characterization. X-ray diffraction (XRD) patterns were recorded using a Rigaku MiniFlex 600 powder diffractometer equipped with a Cu Kα radiation source (40 kV, 15 mA). UV–vis absorption spectra were acquired on a JASCO V-770 spectrometer. Fourier transform infrared (FT-IR) spectra were acquired using a JASCO FT/IR-6600 spectrometer in a diffuse reflectance mode. Scanning electron microscopy (SEM) observations combined with energy-dispersive X-ray spectroscopy (EDS) analyses were performed using a Hitachi SU9000 microscope. Atomic force microscopy (AFM) images were acquired with a Shimadzu SPM-9700 system operated in dynamic mode, using cantilevers with a nominal force constant of 1.7 N m^{-1} (Olympus, OMCL-AC240TS-R3).

X-ray photoelectron spectroscopy (XPS) measurements were carried out using a Shimadzu ESCA-3400 spectrometer. All binding energies were calibrated with reference to the C 1s peak at 285.0 eV. Time-of-flight secondary ion mass spectrometry (TOF-SIMS) measurements were performed using an ION-TOF GmbH TOF-SIMS 5-100-AD instrument.

Preparation of Al_2O_3/NiO electrode. NiO electrodes were prepared according to a previously reported method.[1] Briefly, a precursor solution was prepared by dissolving $Ni(NO_3)_2 \cdot 6H_2O$ (1.0 g, 99.95%, Kanto Chemical) and Pluronic® F-108 (0.5 g, Sigma-Aldrich) in a water/ethanol mixture (4.5 g, w/w = 1:2). The solution was deposited onto fluorine-doped tin oxide (FTO) glass substrates (AXEL, 14 Ω sq^{-1}) by a squeeze-coating method. The films were calcined in air at 773 K for 30 min with a heating rate of 10 K min^{-1}. This deposition–calcination cycle was repeated four times.

Al_2O_3 modification of the NiO electrodes was performed following reported procedures.[2] The NiO films were immersed in aluminum tri-*sec*-butoxide (97%, Sigma-Aldrich) solutions in dehydrated 2-propanol (>99.7%, Kanto Chemical) at 323–333 K for 20 min under an inert atmosphere. The precursor concentration (C_ Al_2O_3) was varied (0.015, 0.15, 1.5, 15, and 150 mM). The films were then hydrolyzed by immersion in water at 323–333 K for 1 min, followed by annealing in air at 723 K for 30 min (heating rate: 10 K min^{-1}), yielding Al_2O_3-modified NiO electrodes (C_Al_2O_3/NiO).

Hybridization of Al_2O_3/NiO electrode and molecule complex. The molecular complexes used in this study are shown in **Fig. S1**. **RuRe**/Al_2O_3/NiO electrodes were prepared via coordination through methylphosphonic acid anchoring groups, following our previous report.[3] Al_2O_3/NiO electrodes were immersed overnight in an acetonitrile solution (4 mL) containing **RuRe** (10 μM). The electrodes were then rinsed with acetonitrile, yielding transparent pale-red films.

Poly-**RuRu′**/Al_2O_3/NiO electrodes were prepared by electrochemical polymerization of vinyl groups according to a previously reported method.[4] First, Al_2O_3/NiO electrodes were immersed in an acetonitrile solution (4 mL) containing a Ru photosensitizer complex bearing both methylphosphonic acid and vinyl groups on the diimine ligands (**RuVP**). After the samples were rinsed with acetonitrile, **RuVP**/Al_2O_3/NiO electrodes were obtained.

Electropolymerization was subsequently carried out in an acetonitrile solution (5 mL) containing a Ru complex with one vinyl-substituted diimine ligand and one non-coordinating diimine ligand (**RuVN^N**, 0.5 mM) and Et_4NBF_4 (0.1 M). A three-electrode configuration was used, with **RuVP**/Al_2O_3/NiO (2.5 cm^2) as the working electrode, a Pt wire as the counter electrode, and an Ag/$AgNO_3$ reference electrode. After the system was purged with Ar for 10 min, cyclic voltammetry was performed between 0 and −1.9 V vs. Ag/$AgNO_3$ at a scan rate of 200 mV s^{-1} for 20 cycles. The resultant electrodes were washed with acetonitrile to obtain *poly*-**Ru**/Al_2O_3/NiO. Finally, the electrodes were immersed overnight in an acetonitrile solution (4 mL) containing a Ru catalyst complex ($[Ru(CO)_2Cl_2]_n$, 0.5 mM), affording *poly*-**RuRu′**/Al_2O_3/NiO electrodes.

Photoelectrochemical measurements. Photoelectrochemical measurements were conducted at room temperature using a potentiostat (Hokuto Denko, HSV-110) and a single-compartment electrochemical cell made of Pyrex glass. A three-electrode configuration consisting of the prepared electrode as the working electrode (irradiated area: 2.5 cm^2), a Pt wire counter electrode, and an Ag/AgCl reference electrode (saturated KCl aqueous solution) was used.

An aqueous $NaHCO_3$ solution (50 mM, 99.5%, Kanto Chemical) saturated with CO_2 by bubbling for at least 30 min (pH 6.6) was used as the electrolyte. A 300 W Xe lamp (Asahi Spectrum, MAX-303) equipped with an IR-blocking mirror module and either a band-pass filter (MX0460, λ = 460 nm) or cutoff filters (HOYA Y48, λ > 460 nm) was used as the light source. All electrode potentials were converted to the reversible hydrogen electrode (RHE) scale using the following equation:

$E_{RHE} = E_{Ag/AgCl} + 0.059\ pH + 0.197$ at 298 K

The incident photon-to-current efficiency (IPCE) was calculated according to

$IPCE\ (\%) = [(1240/\lambda_{ex})\ (I_{light} - I_{dark})/P_{light}] \times 100$

where λ_{ex} (nm) and P_{light} (μW cm^{-2}) are the wavelength and power density of the incident light, respectively, and I_{light} and I_{dark} (μA cm^{-2}) are the current densities under illumination and in the dark, respectively.

Mott–Schottky measurements were performed using a potentiostat (Hokuto Denko, HZ-Pro) under the same photoelectrochemical conditions.

Photoelectrochemical CO_2 reduction. Photoelectrochemical CO_2 reduction experiments were carried out using a Pyrex H-type cell separated by a Nafion 117 membrane (Sigma-Aldrich). The photocathode and Ag/AgCl reference electrode were placed in the cathodic compartment, and a Pt wire counter electrode was placed in the anodic compartment. The photocathode was irradiated with light in the wavelength range 460 < λ < 650 nm using a 300 W Xe lamp (Asahi Spectrum, MAX-303) equipped with an IR-blocking mirror and a cutoff filter (HOYA Y48). Gaseous products (CO and H_2) were quantified using a micro-gas chromatograph (Inficon, MGC3000A), and formate ($HCOO^-$) in the electrolyte was analyzed by capillary electrophoresis (Agilent 7100, Otsuka Electronics; detection limit ≈ 50 nmol in 15 mL).

Operando transient absorption spectroscopy. Operando transient absorption measurements were performed using a homemade spectroelectrochemical cell. An Nd:YAG laser system (EKSPLA, NT242) equipped with an optical parametric oscillator (OPO) was used to generate excitation pulses at λ_{ex} = 420 nm. White-light probe pulses (400–500 nm) were generated by focusing the second harmonic (515 nm) of a Yb:KGW regenerative amplifier onto a sapphire crystal. The transmitted probe light was dispersed by a polychromator (JASCO, CT-10) and detected using a multichannel CMOS detection system (UNISOKU, USP-PSMM-NP). Temporal delays were controlled using a delay/pulse generator (Stanford Research Systems, DG535). The rate constants were determined from the data by least-squares fit using a convolution function of a Gaussian function and a double exponential function. To eliminate anisotropy effects, the polarization angle between the excitation and probe beams was set to the magic angle. The electrochemical conditions were identical to those used for photoelectrochemical measurements, and a potential of –0.7 V vs. Ag/AgCl was applied using a potentiostat (BAS, ALS600E).

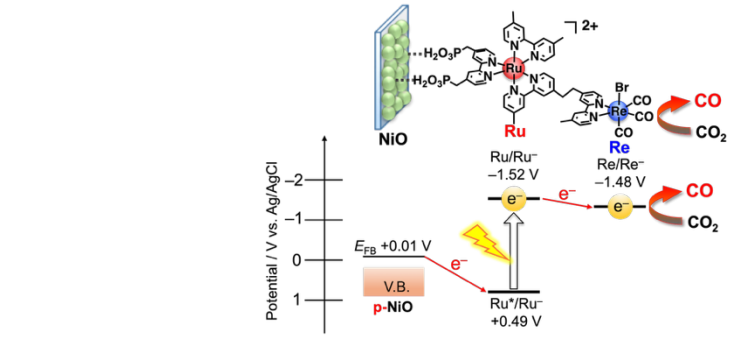

Scheme S1. Photoelectrochemical CO_2 reduction using a RuRe/NiO hybrid photocathode.

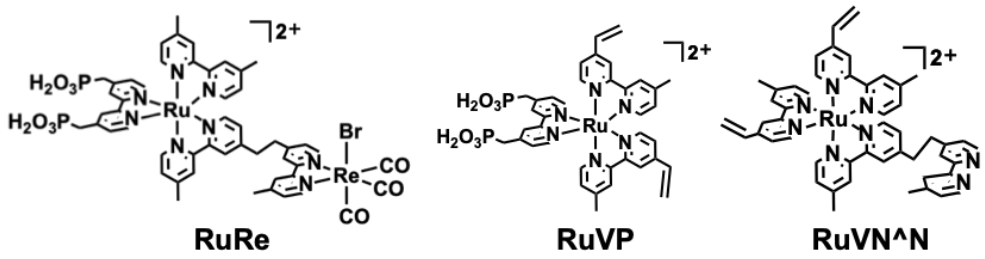

Fig. S1. Structures and abbreviations of the metal complexes used in this work.

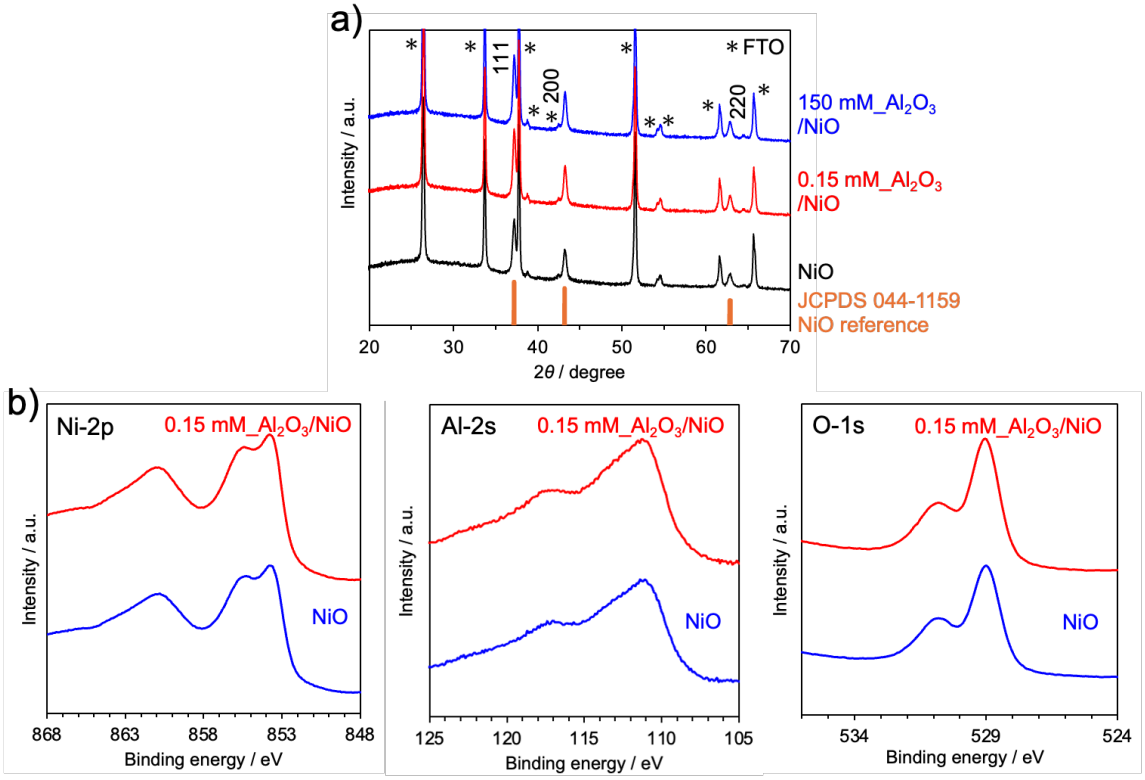

Fig. S2. a) XRD patterns of 150 mM_Al_2O_3/NiO, 0.15 mM_Al_2O_3/NiO, and NiO and b) Ni-2p, Al-2s, and O-1s XPS spectra of 0.15 mM_Al_2O_3/NiO/FTO and NiO/FTO.

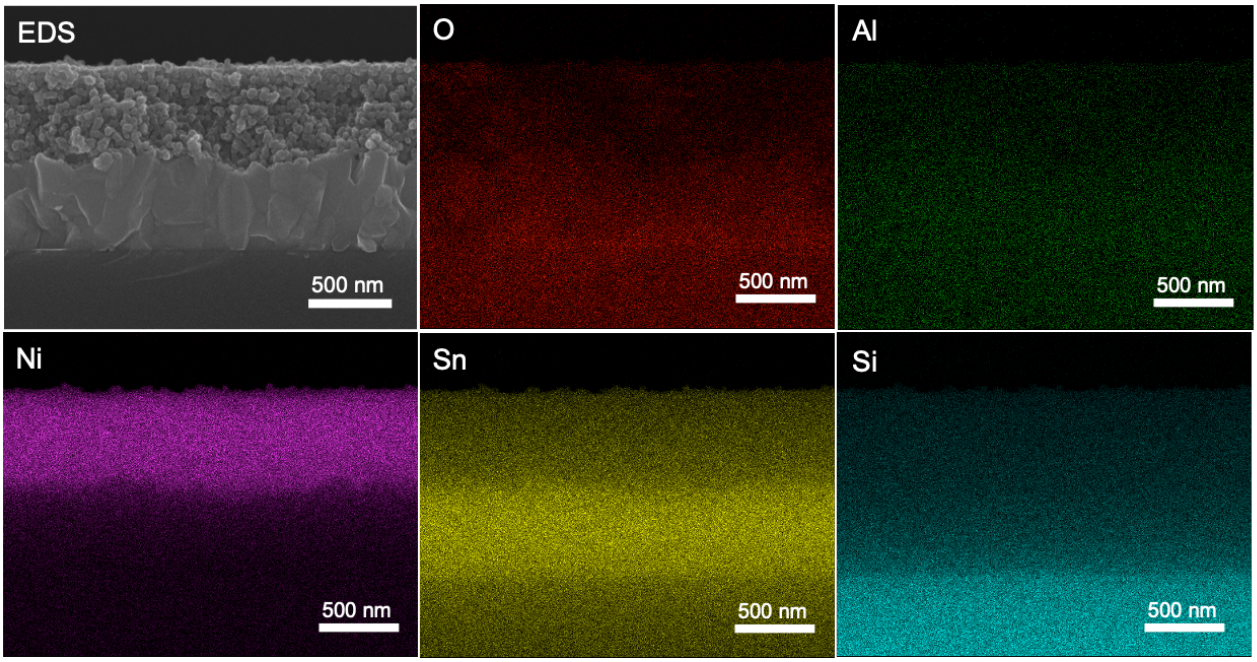

Fig. S3. EDS mapping analysis of 0.15 mM_Al_2O_3/NiO.

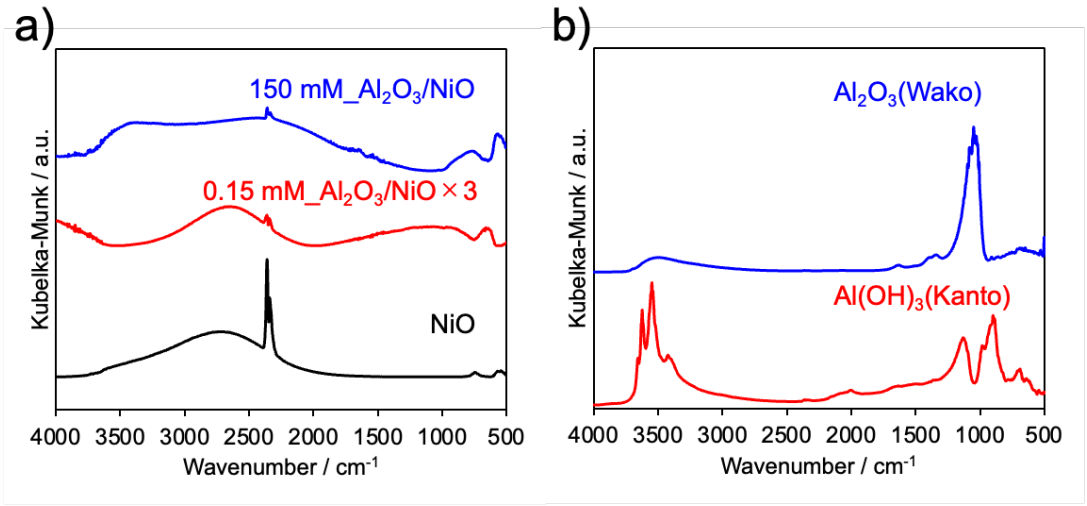

Fig. S4. a) FT-IR spectra of 150 mM_Al_2O_3/NiO, 0.15 mM_Al_2O_3/NiO, and NiO. Panel b) shows the spectra of Al_2O_3 (Wako) and $Al(OH)_3$ (Kanto) references.

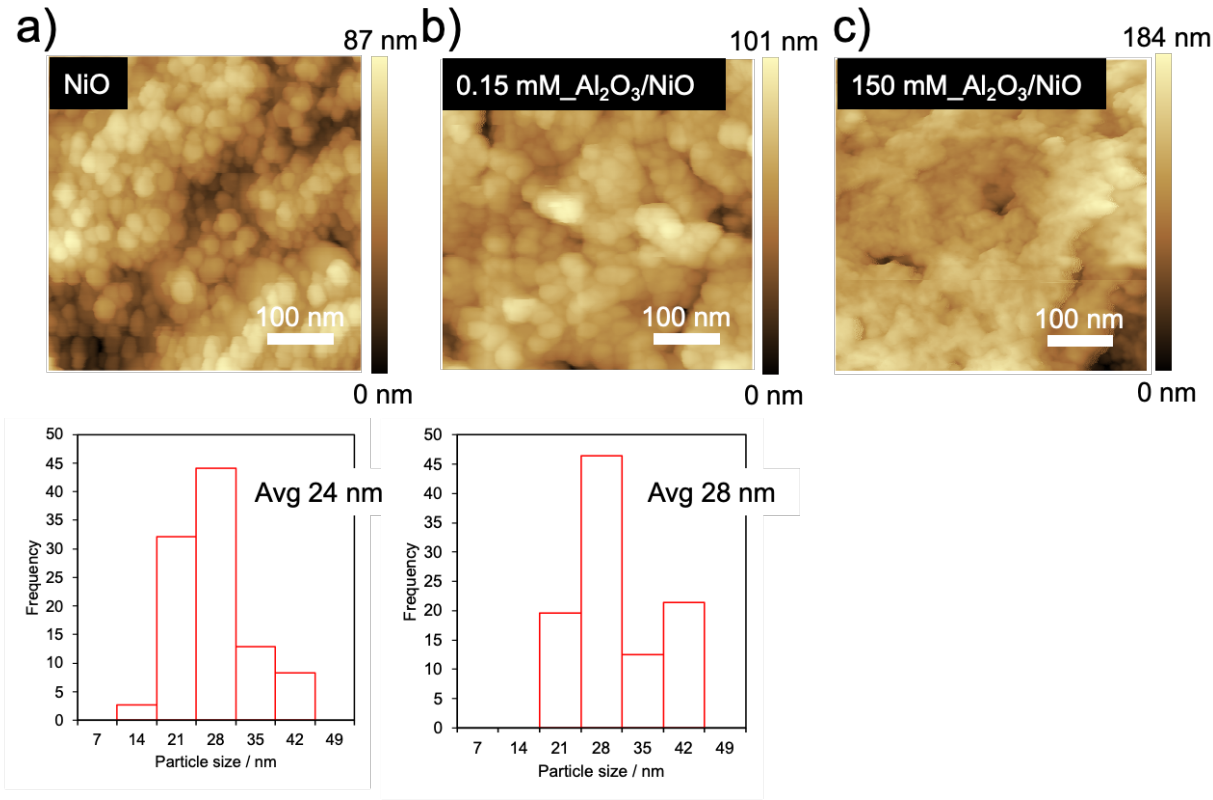

Fig. S5. a–c) AFM images of the NiO/FTO, 0.15 mM_Al_2O_3/NiO/FTO, and 150 mM_Al_2O_3/NiO/FTO. Particle size distributions estimated from the AFM images are also shown.

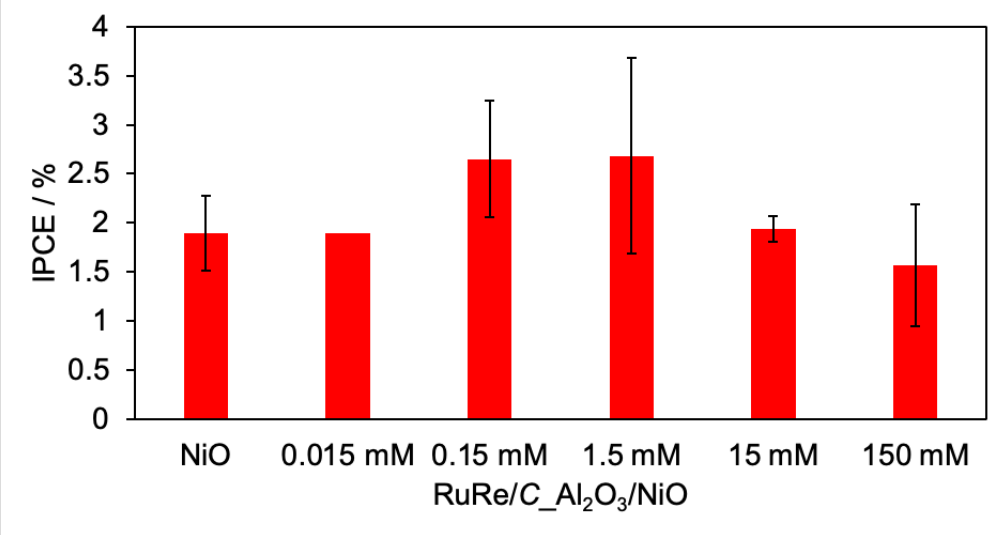

Fig. S6. IPCEs of **RuRe**/*C*_Al_2O_3/NiO prepared with different *C* values. IPCEs were calculated from current–time curves (scan rate, 10 mV s^{-1}) recorded in 50 mM aqueous $NaHCO_3$ electrolyte under a CO_2 atmosphere (pH 6.6) at –0.7 V vs. Ag/AgCl under 460 nm irradiation (2 mW cm^{-2}) (*C* = 0 mM means unmodified **RuRe**/NiO). These IPCE measurements were used to identify the optimal modification conditions prior to performing controlled-potential electrolysis experiments. Because the photocurrent density under photoelectrochemical conditions directly reflects the rate of product formation,[4, 5] these measurements provide a reliable comparison of catalytic activity among samples.

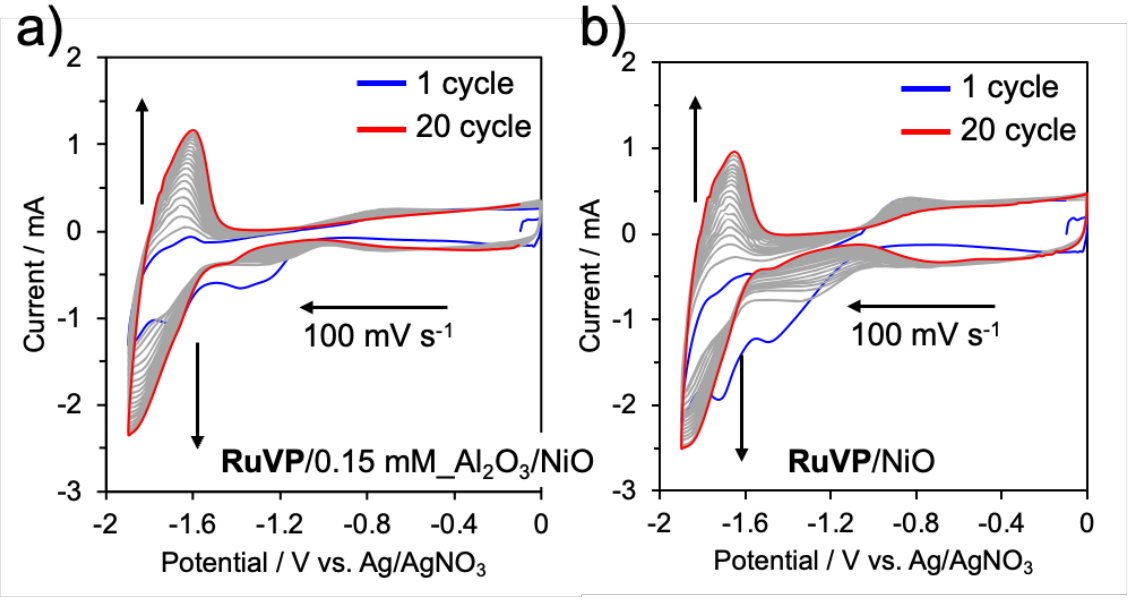

Fig. S7. Cyclic voltammograms acquired during electropolymerization of **RuVN^N** on a) **RuVP**/Al_2O_3/NiO/FTO and b) **RuVP**/NiO/FTO (electrode area, 2.5 cm^2) in an Ar-saturated acetonitrile solution containing **RuVN^N** (0.5 mM) and Et_4NBF_4 (0.1 M) as an electrolyte. The potential was repeatedly applied (20 times) between 0 and −1.9 V at a scan rate of 100 mV s^{-1}. Note that the oxidation–reduction wave in the region from –0.8 to –1.6 V is attributed to the redox of Ni^{3+}/Ni^{2+}.[3]

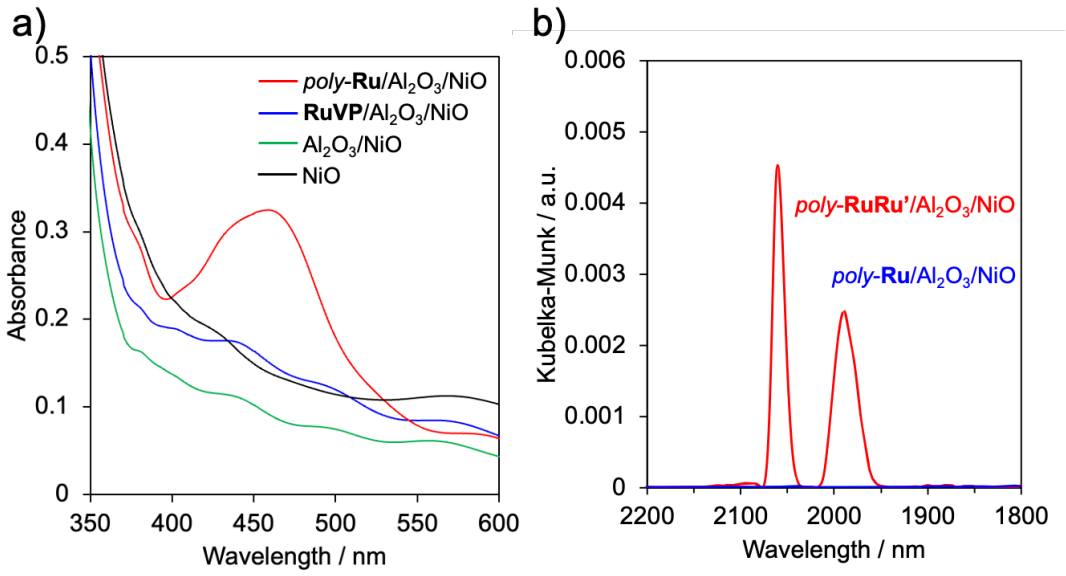

Fig. S8. Hybridized molecular photocatalyst characterization. a) UV-vis spectra and b) FT-IR spectra of NiO and 0.15 mM_Al_2O_3/NiO electrodes prepared under various conditions.

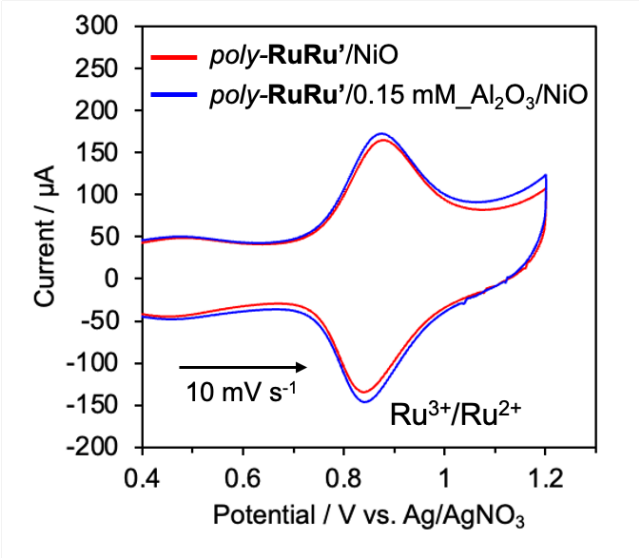

Fig. S9. Cyclic voltammograms on *poly*-**RuRu′**/0.15 mM_Al_2O_3/NiO/FTO and *poly*-**RuRu′**/NiO/FTO (electrode area, 2.5 cm^2) in an Ar-saturated acetonitrile solution containing Et_4NBF_4 (0.1 M) as an electrolyte between 0 and +1.2 V at a scan rate of 10 mV s^{-1}. Note that the oxidation–reduction wave in the region from +0.7 to +1.0 V is attributed to the redox of Ru^{3+}/Ru^{2+}.[3]

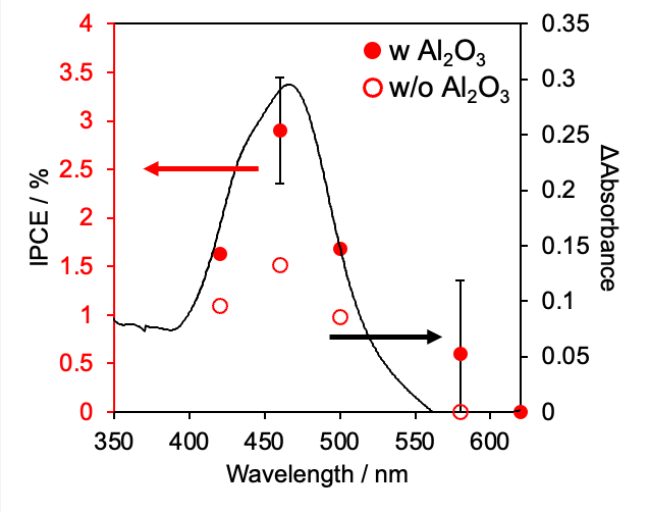

Fig. S10. Action spectra of *poly*-**RuRu′**/0.15 mM_Al_2O_3/NiO (w Al_2O_3) and *poly*-**RuRu′**/NiO (w/o Al_2O_3) calculated from current–time curves (scan rate, 10 mV s^{-1}) under intermittent visible-light irradiation (2 mW cm^{-2}, λ = 460 nm). The black line represents the UV–vis spectrum of *poly*-**RuRu′**/0.15 mM_Al_2O_3/NiO after the absorbance of the NiO electrode was subtracted.

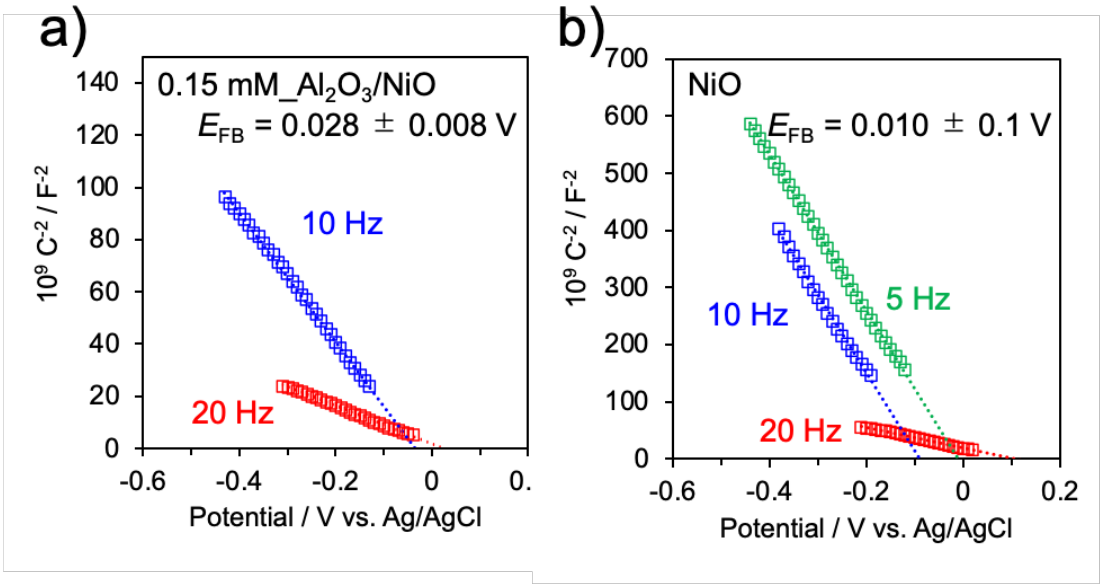

Fig. S11. Mott–Schottky plot of a) 0.15 mM_Al_2O_3/NiO/FTO and b) NiO/FTO (electrode area, 2.5 cm^2) recorded at various frequencies in 50 mM $NaHCO_3$ aqueous solutions under a CO_2 atmosphere.

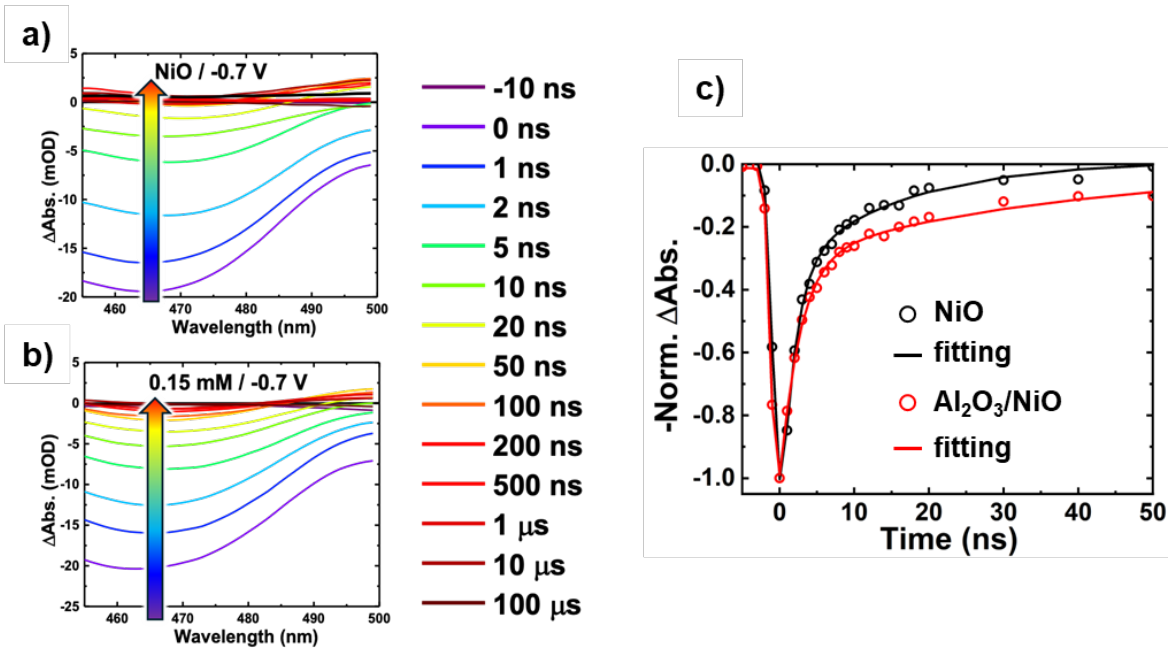

Fig. S12. Transient absorption spectra of a) *poly*-**RuRu′**/NiO and b) *poly*-**RuRu′**/0.15 mM_Al_2O_3/NiO photocathodes measured at –0.7 V vs. Ag/AgCl in CO_2-saturated 50 mM $NaHCO_3$ aqueous solutions using 420 nm laser excitation. c) Recovery profiles at 465 nm and fitting functions of the transient absorption spectra.

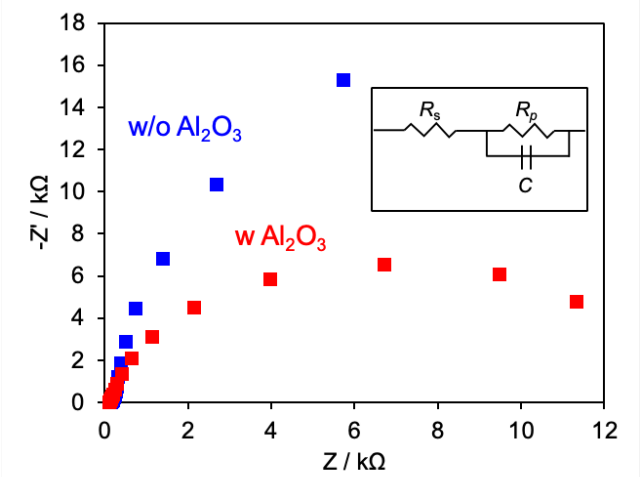

Fig. S13. Nyquist plots for *poly*-**RuRu'**/0.15 mM_Al_2O_3/NiO (w Al_2O_3) and *poly*-**RuRu'**/NiO (w/o Al_2O_3). The plots were acquired at room temperature at open circuit voltage under visible light (32 mW cm^{-2}; $\lambda > 460$ nm; irradiation area, 2.5 cm^2). The frequency range measured was $2.0\times10^5 \sim 0.1$ Hz and the amplitude of voltage was 10 mV. Inset: the equivalent circuit used for data fitting (R_s: solution resistance and R_p: charge-transfer resistance). The measurements were conducted in 50 mM $NaHCO_3$ aqueous solution under a CO_2 atmosphere (pH 6.6). The semicircle observed in the Nyquist plots corresponds to R_p. Upon Al_2O_3 modification, the semicircle becomes smaller, indicating a decrease in the interfacial charge-transfer resistance. This result is consistent with improved interfacial charge-transfer processes in the presence of the Al_2O_3 layer by blocking undesirable back electron transfer paths.

Table S1. Adsorption amount of **RuRe** and IPCEs of **RuRe**/*C*_Al_2O_3/NiO and **RuRe**/NiO under intermittent visible-light irradiation (2 mW cm^{-2}, $\lambda = 460$ nm)

C / mM	The adsorption amount of **RuRe** / nmol	IPCE / %
0	22.2	1.9±0.4
0.015	14.7	1.9
0.15	19.0	2.7±0.6
1.5	21.0	2.7±1.0
15	23.6	1.9±0.1
150	25.6	1.6±0.6

Table S2. Results of CO_2 reduction of *poly*-**RuRu'**/0.15 mM_Al_2O_3/NiO and *poly*-**RuRu'**/NiO[a]

Sample	Amount of products / μmol (Faradaic efficiency)[b]			
	CO	HCOOH	H_2	Total
poly-**RuRu'**/0.15 mM_Al_2O_3/NiO	2.1 (43.1)	1.3 (27.0)	0.2 (4.8)	3.6 (74.9)
poly-**RuRu'**/NiO	0.6 (30.0)	0.6 (29.3)	0.1 (5.0)	1.3 (64.4)
poly-**RuRu'**/0.15 mM_Al_2O_3/NiO[c]	n.d.	n.d.	n.d.	n.d.

[a] The measurement conditions are the same as in Fig. 2. [b] Total product amount after 5 h irradiation. [c] Ar atmosphere.

References

1. S. Sumikura, S. Mori, S. Shimizu, H. Usami and E. Suzuki, *J. Photochem. Photobiol. A: Chem.*, 2008, **199**, 1–7.
2. E. Palomares, J. N. Clifford, S. A. Haque, T. Lutz and J. R. Durrant, *J. Am. Chem. Soc.*, 2003, **125**, 475–482.
3. G. Sahara, R. Abe, M. Higashi, T. Morikawa, K. Maeda, Y. Ueda and O. Ishitani, *Chem. Commun.*, 2015, **51**, 10722–10725.
4. R. Kamata, H. Kumagai, Y. Yamazaki, M. Higashi, R. Abe and O. Ishitani, *J. Mater. Chem. A*, 2021, **9**, 1517–1529.
5. G. Sahara, H. Kumagai, K. Maeda, N. Kaeffer, V. Artero, M. Higashi, R. Abe and O. Ishitani, *J. Am. Chem. Soc.*, 2016, **138**, 14152–14158.